An improved electrokinetic method to consolidate porous materials

Feijoo, Jorge; Ottosen, Lisbeth M.; Nóvoa, X. R.; Rivas, Teresa; de Rosario, Iván

Published in:
Materials and Structures

Link to article, DOI:
10.1617/s11527-017-1063-1

Publication date:
2017

Document Version
Peer reviewed version

Materials and Structures

An improved electrokinetic method to consolidate porous materials

--Manuscript Draft--

Manuscript Number:	MAAS-D-17-00269R1
Full Title:	An improved electrokinetic method to consolidate porous materials
Article Type:	Original Research
Keywords:	Sandstone; electrokinetic technique; consolidation; salts; water, cultural heritage.
Corresponding Author:	Jorge Feijoo, PhD Universidade de Vigo Vigo, Pontevedra SPAIN
Corresponding Author Secondary Information:	
Corresponding Author's Institution:	Universidade de Vigo
Corresponding Author's Secondary Institution:	
First Author:	Jorge Feijoo, PhD
First Author Secondary Information:	
Order of Authors:	Jorge Feijoo, PhD
	L.M. Ottosen, PhD
	X.R. Nóvoa, PhD
	T. Rivas, PhD
	I. de Rosario, PhD student
Order of Authors Secondary Information:	
Funding Information:	Ministerio de Educación, Cultura y Deporte (FPU grant) — Mr. Jorge Feijoo
Abstract:	Consolidation is considered one of the major restoration treatments applied on cultural heritage. This kind of treatment is focused on to preserve the external weathered layers of stone reducing their degradation caused by external alteration agents (mainly water and soluble salts). However the consolidation using commercial products have some limitations, such as: 1) low penetrability; 2) no chemical and mineralogical affinity with the material to treat and 3) release of toxic compounds (VOCs), during the solvent evaporation. In the last years, a new consolidation method based on electrokinetic techniques was developed. This method allows filling some pores by the precipitation of an inorganic compound. As a result the method allows increasing the penetration depth of current consolidation treatments. However, this method needs to be improved since: 1) no special care is taking in controlling the pH of the solutions in contact with the porous material, which can damage it and 2). It is difficult to determine in which area the consolidation takes place. In this study an electrokinetic consolidation method, which has two steps between which the current is reversed, is proposed to solve all of these problems. The results show that the proposed treatment achieves better results in terms of penetrability and durability of current consolidation treatments, and moreover prevent that the treated material to be exposed to extreme pH values.
Response to Reviewers:	Dear Editor in Chief Firstly we would like to thank the comments of the reviewers and their opinion about the possible interest that this paper could cause for the audience of Materials and Structures.

	However, the improvement of the stone looks like not so much. I hope you to try the method to be better. AUTHORS: Certainly these are the preliminary results that we have obtained with this new procedure. However we are working on optimizing the procedure (different solutions, types of current, etc.) in order to improve it. Currently I am finalizing a paper where it is shown that this treatment allows to greatly increasing the uniaxial compressive strength of porous materials (in this case granite samples) due to the reduction in the pore volume that takes place over a large area. Also, I myself do not understand DDE, and I hope you will implement exposure test in the targeted natural (weather) conditions. AUTHORS: The durability parameter DDE is a mathematical method to estimate the durability of a material against the action of external alteration agents from the data of its porous structure. The correlation between the DDE estimator and the results obtained after accelerated alteration test (resistance to salt crystallization) was demonstrated in some studies. Currently we are working on a paper that analyzes the durability of this treatment against some accelerated alteration tests and we are also evaluating the technique in a pilot structure exposed to weathering conditions. We would like to again express our gratitude to both reviewers and we hope that now this work meets the necessary conditions to be published in this journal and can thus be reported in the scientific community
Additional Information:	
Question	**Response**
Provide the total number of words in the manuscript (excluding figure caption and table caption)?	7997
Provide total number of FIGURES?	13
Provide total number of TABLES?	2

An improved electrokinetic method to consolidate porous materials

Jorge Feijoo*

Ph.D. Dep. Ingeniería de los Recursos Naturales y Medio Ambiente, Universidad de Vigo, Lagoas-Marcosende s/n, 36310 Vigo, Spain. jfeijoo@uvigo.es

L.M. Ottosen

Department of Civil Engineering Building 117, Technical University of Denmark, 2800 Kgs. Lyngby, Denmark. *lo@byg.dtu.dk*

X.R. Nóvoa

Ph.D. Dep. Chem. Eng., ENCOMAT group, EEI. University of Vigo. 36310 Vigo-Spain, Lagoas-Marcosende s/n, 36310 Vigo, Spain. rnovoa@uvigo.es

Teresa Rivas

Ph.D. Dep. Ingeniería de los Recursos Naturales y Medio Ambiente, Universidad de Vigo, Lagoas-Marcosende s/n, 36310 Vigo, Spain. trivas@uvigo.es

Iván de Rosario

Ph.D. Student Dep. Ingeniería de los Recursos Naturales y Medio Ambiente, Universidad de Vigo, Lagoas-Marcosende s/n, 36310 Vigo, Spain. irosario@uvigo.es

** Corresponding author*

Abstract

Consolidation is considered one of the major restoration treatments applied on cultural heritage. This kind of treatment is focused on to preserve the external weathered layers of stone reducing their degradation caused by external alteration agents (mainly water and soluble salts). However the consolidation using commercial products have some limitations, such as: 1) low penetrability; 2) no chemical and mineralogical affinity with the material to treat and 3) release of toxic compounds (VOCs), during the solvent evaporation.

In the last years, a new consolidation method based on electrokinetic techniques was developed. This method allows filling some pores by the precipitation of an inorganic compound. As a result the method allows increasing the penetration depth of current consolidation treatments. However, this method needs to be improved since: 1) no special care is taking in controlling the pH of the solutions in contact with the porous material, which can damage it and 2). It is difficult to determine in which area the consolidation takes place.

In this study an electrokinetic consolidation method, which has two steps between which the current is reversed, is proposed to solve all of these problems. The results show that the proposed treatment achieves better results in terms of penetrability and durability of current consolidation treatments, and moreover prevent that the treated material to be exposed to extreme pH values.

Keywords

Sandstone; electrokinetic technique; consolidation; salts; water, cultural heritage.

1. Introduction

The preservation of infrastructures, especially those built with porous materials such as ornamental rocks, is a major problem in materials conservation. Durability of porous materials used in building construction depends on extrinsic factors to the material, i.e., factors beyond the material, which can have influence in their conservation state. Also intrinsic factors are important to the durability, i.e., factors that depend on the material itself, such as its chemical and

mineralogical composition, their mechanical and thermal properties and its porosity and pore system among others. The conjunction of these two factors determine the mechanism of alteration, which affect the material and will have influence in their future sustainability [1].

Among the intrinsic factors it is necessary highlight the role of porosity, especially: 1) the accessible porosity: parameter related with the capacity of the material to allow the ingress of water and the external aggressive agents into the material and in addition to condition their mobilization through it [1]. 2) the shape and size of the porous system, which influences in the greater or lesser harmful effect that can generate the internal pressures caused by alterations agents such as those caused by the freeze-thaw of water or by salt crystallization [2-3]. Moreover it is necessary to highlight that the pores (both the open and the closed) have negative effects in the geomechanical properties of a material. They reduce the resistance against mechanical stresses and they act as stress concentrators favouring the onset of breaking through them [4].

Among the extrinsic factors of deterioration are the entrance of water and the presence of soluble salts in the pores. The joint action of these two is especially dangerous as stated in [5]. Water can cause: 1) *chemical alteration* by dissolution (mainly on carbonated rocks such as sandstone, limestone or marble), hydration (mainly affects to evaporitic rocks such as anhydrite) or hydrolysis (which affects mainly to silicated stones such as granite) [6]. 2) *physical alteration* due to a) the expansion-contraction that occurs during the cyclical processes of humidity-dryness, which can cause the fatigue of a rock; b) the reduction of the cohesion of the rock due to the water adsorbed on the surface of the grains reduces its cohesion by the interfacial water-surface energy of the mineral [7]. c) The capillary pressure generated in rocks partially saturated due to the interfacial tension between the surface of the pores, liquid water, and air. The value of this pressure depends on the pore size and environmental relative humidity [8]; d) frost damage caused by the pressure in the pores when water increase the volume by 9% during freezing [9-10]. In addition to the chemical and physical alterations, water favours the growth of microorganisms and higher plants that promotes physico-chemical alteration processes [11].Water also encourages and promotes the transport of other harmful agents such as soluble salts.

Soluble salts tend to crystallize within the pores of the material, especially in those that are close to the evaporation surfaces [1-2], as they are transported to this area with the front moisture, during the drying process [12-13]. During crystallization, some salts are able develop pressures that exceed the tensile strength of the material, increasing the size of the pores by formation of micro-cracks and thereby making the material more porous and more prone to new alteration processes. These pressures are usually higher than the freeze-thaw pressures [14].The deterioration due to presence of soluble salts is associated with the periodic changes in their state, i.e. crystallization-dissolution cycles. For this reason, many of the intervention strategies that are applied to monuments are based on keeping the humidity out and/or to keep temperature and relative humidity conditions constant in order to ensure that the salts do not change their state. However the size of the monuments and the influence of environmental conditions make the application of these intervention strategies difficult and inefficient.

Different methods to hinder moisture penetration into a structure have been developed. The main entrance of water into the structure is through the soil by capillary suction [15] and also infiltration by rainwater [16]. In order to limit the amount of water rising by capillary suction into the porous material, the current techniques used are [15]: 1) the construction of sub-soil drains around the monument in order to reduce the water flux that can ingress; 2) creation of arches in the wall to reduce the section of entrance; 3) wall cutting and the injection of water repellents or other chemical products to create a chemical barrier. These three techniques are focused on reduce the wall sorptivity. Other techniques are: 4) the application of systems focused on increasing the evaporation capacity of the wall (Knapen tubes, wall base ventilation, thermal method, etc.); 5) electrokinetic methods focused on removal the water towards the ground level by electro-osmosis. However, most of these techniques have several limitations and drawbacks such as low efficacy or potential damage to the treated material. It is therefore essential to develop new techniques in order to limit the ability of water absorption of the material without causing damage that could endanger the value of the structure.

Regarding the removal of salts, there are currently different desalination techniques, such as immersion baths [17], the application of poultices [18-19], the use of crystallization inhibitors [20] and the use of electrokinetic techniques [21-22]. Of these methods, the electrokinetic techniques are the most effective since, as shown in [23-24], they allow to reduce the ionic content present in rock to very low contents in a short treatment time.

A common conservation practice carried out on damaged and fragile monuments is the application of consolidating products aiming at minimizing the loss of material. There are many commercial consolidation products. These products are broadly classified as described in [25]: inorganic materials, organic materials, alkoxysilanes (broadly use in the field of building intervention [26-27]), and nano-materials with consolidant effect [28]. The consolidation actions aim to improve the adhesion of unbound mineral grains with the part of the porous material not yet damaged. Thus, attempting to fill the empty spaces present in the material to be treated. Furthermore, the consolidation can slightly increase the mechanical properties of the material due to the reduction of the pore volume fraction [25].

However, there are several disadvantages and/or limitations in the present consolidation treatments, such as:

- Low penetrability into the stone substrate, which depends on the consolidant properties (chemical composition, viscosity, surface tension), stone properties (porosity distribution, water absorption, capillary suction) as well as the way of application [29-33]. The consolidation of the altered material, with low cohesion, onto the healthy material is often limited by the low penetrability.
- Low durability, due to the high rate at which the consolidating compounds are degraded, which is a problem mainly when organic consolidants are used [34].
- Low increase in mechanical properties due to the low penetrability of the consolidant.
- Reduction of the vapour permeability of the treated surface of the porous material. This reduction is caused by the clogging only of the pores present close to the evaporation

surfaces of the material. This fact can increase the alteration damage caused by the soluble salts, which penetrate from the internal layers of material and cannot be transported to the surface, thus tending to precipitate in the material as sub-efflorescence [28, 35].

- Release of toxic compounds (VOCs: white spirit, acetone, toluene, xylene, etc.), to humans and the environment, during the solvent evaporation [36].

In recent years, scarce scientific researches focused on the application of electrokinetic techniques in order to consolidate or protect stones in cultural heritage have arisen [37-38]. In [37], Meloni et al. promoted, by means this technique, the artificial generation of a protective whewellite ($CaC_2O_4 \cdot H_2O$) coating on the surface of a marble. The method developed in this study is based on the application of an electric current into a solution in which the samples (in this case marble samples) are immersed. Therefore this technique presents as a limitation the size of the samples to be treated. In [38], Bernabeu et al. developed a method for consolidate porous materials by means the application of an electric DC field throughout the whole rock herein transporting the ions present in an anolyte and catholyte into the material. As a result, precipitation of an inorganic compound, with low solubility in water, occurs in certain pores. This precipitation occurs when the concentration of both ions (forming the solid precipitation product) is higher than the concentrations established by the solubility product. As stated in [38], this new technique allows to increase the penetration depth of current consolidation treatments. However, in that study no special care was taking in controlling the pH of the solutions in contact with the porous material to be treated. Extreme pH values (both acid and alkaline) can cause new chemical alteration damage in certain materials, and should thus be prevented. Furthermore, these pH values could significantly decrease the effectiveness of the treatment, hindering the formation of the precipitation product. Another limitation relates to the consolidation process, since it is only possible to achieve pore blocking in a particular area, which may be superficial or deep, leaving the rest of the material without precipitated consolidant.

The present study shows an optimization of the electrokinetic consolidation treatment which allow: 1) increasing the pore blocking area, allowing consolidation of both superficial and deep

pores, which will reduce the water sorptivity of the material, and as a consequence durability increases; 2) avoiding the extreme pH environments in the vicinity of the material to be treated.

2. Material and Methods

2.1. Stone used

A very fine-grained yellow sandstone was used. This stone was used in the construction of Kronborg Castle located in the Oresund's Strait (Denmark) and was used also in previous studies [12, 24].

The chemical, mineralogical and textural properties were determined by X-ray fluorescence (Sequential X-ray Spectrometer Siemens SRS 3000), X-ray diffraction (Siemens D5000 diffractometer) and SEM-EDX (Phillips XL 30) respectively. The main physical properties of the sandstone were determined using European standards. The pore size distribution was determined by mercury intrusion porosimetry using an AutoporeIV9500 porosimeter of Micromeritics. This porosimeter has two ranges of working pressure, one range of high pressure between 0.20MPa-225MPa and another of low pressure between 14kPa-0.20Mpa, thus allowing the characterization of the pores with an access diameter between 116μm-3.8nm.

From data provided by the porosimeter, the tortuosity of the pores network was estimated in an indirect way using eq. 1 proposed by [39] and used in [24]. This parameter gives an estimate of the real distance that a liquid must travel with respect to the straight line path.

$$\tau = V_i / (V_i - V_e) \quad (1)$$

In Eq. 1 V_i represents the total mercury intruded, and V_e the total mercury extruded, both in mL/g.

The charge at pore network walls (zeta potential), was calculated using a Zetasizer Nano Z, from Malvern Instruments.

Finally, durability of the stone was estimated using the mathematic estimator DDE proposed in [40]. This parameter defines the capacity of a certain material to resist and maintain the original size, shape, mechanical properties and aesthetic appearance over time. It is closely related with

the balance of water present inside the stone and the accompanying alteration processes, such as the action of soluble salts [41]. DDE is calculated in function of the distribution of pore sizes and porosity, according to eq. 2.

$$DDE(\mu m^{-1}) = \sum(D_v (r_i) / r_i) \, Pa \quad (2)$$

where, D_v is the pore size distribution for each pore ri (in parts per unit); r_i the pore size in µm; and Pa the accessible porosity in parts per unit. In this study Pa used is the accessible porosity to mercury.

To calculate DDE, the following pore size intervals (in µm) proposed by [42] was considered: <0.01; 0.01 to 0.1; 0.1 to 1; 1 to 10 and 10 to 100. The central values of these intervals are respectively as stated [40]: 0.00316, 0.0316, 0.316, 3.16 and 31.6 µm.

In all these cases, the higher the value of the proposed DDE estimator, the lower the durability exhibited by the material against the pressures exerted by crystallization of salts or freeze-thaw cycles [40].

2.2. Electrokinetic Setup

Figure 1 shows a cross section of the experimental device employed. To apply the procedure, an electrode compartment is placed on each side of the stone: anodic and cathodic compartments. Both compartments consists of three sections (M1 to M3) separated by cellulose filters. The M1 and M3 sections contain a solution (DA is the solution at the anode and DC at the cathode), while the M2 sections in each compartment is filled with a poultice (PA is the poultice at the anode and PC at the cathode). The use of cellulose filters in order to separate the compartments filled with poultices to those filled with solutions prevents the decomposition of the structure of the poultices and in consequence, their spreading into the solutions. Furthermore, placing the poultices between the two solutions allows to hydrate the poultice during the treatment, and hereby hinder drying of the poultice, which could hinder passage of electric current (ionic flow).

INSERT FIGURE 1

The solutions DA (at the anode) and DC (at the cathode), in the sections M1 and M3 at each side of the stone, must contain the ions responsible for clogging the stone pores during the treatment. DA provides the cation of the inorganic consolidant, and DC provides the anion. The treatment can be adapted to different porous materials, as it allows selecting different solutions (DA and DC) for each specific case, in order to obtain the inorganic consolidant with a good mineralogical affinity with the porous material.

In this specific case, consolidation of sandstone, sections M1 and M3 were filled with solution DA (0.5 M magnesium acetate, pH 8.9) in the anode compartment. In the cathode compartment sections M1 and M3 were filled with solution DC (0.5 M ammonium carbonate, pH 8.9). When applying the electric field, the cation Mg^{2+} is supplied to the stone from the anode side and the anion CO_3^{2-} from the cathode side. Hereby supplying the ions to precipitate the consolidant $MgCO_3$, in the anhydrous state or in some of its hydration states.

The first section (M1), holds also the electrodes. The electrodes employed were titanium made, i.e. they were inert and thus acting just as support of the processes. Electrolysis at the electrodes will be responsible for the production of ions at the electrode surfaces. Electrolysis will cause an acidic environment in the solution in section M1at the anode according to Eq. 3, and an alkaline environment in M1 at the cathode according to Eq. 6.

Reactions in the anodic compartment

Electrochemical: $$H_2O \longrightarrow 2H^+ + \frac{1}{2}O_{2(g)} + 2e^- \quad (3)$$

Chemical: $$MgCO_3 + H^+ \longrightarrow Mg^{2+} + HCO_3^- \quad (4)$$

Chemical: $$HCO_3^- + H^+ \longrightarrow CO_{2(g)} + H_2O \quad (5)$$

Reactions cathodic compartment

Electrochemical: $$2H_2O + 2e^- \longrightarrow 2OH^- + H_{2(g)} \quad (6)$$

During the electrokinetic treatment, it is necessary to maintain pH between 6.5 to 8.5 in the solution located in M3 section (next to the stone) in order to avoid a chemical alteration of the stone. Furthermore, the existence of extreme pH values in the vicinity of the porous material could hinder the precipitation of the inorganic consolidant. To buffer the extreme pH environments, caused by electrolysis at the electrodes, an intermediate section (M2) filled with a pH buffering poultice, is placed between the electrode section M1 and solution M3. In the anodic compartment the poultice (PA) was made of kaolin, magnesium carbonate, and ultrapure water in a proportion 1:2:6 by weight. The role of this medium is to hinder the acid solution from the anode in reaching the stone. Decomposition of this poultice occurs according to Eqs. 4, 5. During the buffering process a supply Mg^{2+} cations migrating towards the cathode occurs.

In the cathode compartment the buffering (PC) was kaolin and ultrapure water in a proportion 1.5:1 by weight. The use of kaolin in this compartment is justified because kaolin has a high ion exchange capacity. This high ion exchange capacity allows retaining the OH^- groups formed at the cathode, as demonstrated in [12, 23-24], preventing therefore the alkalization from the cathode to reach the stone.

In order to minimize the evaporation of both dissolutions through the lateral faces of the samples, these were wrapped carefully with PVC film.

2.3. Electrokinetic consolidation procedure

The electrokinetic consolidation procedure used in this study comprises two steps (called respectively CT1 and CT2), during both a constant voltage of 10V is applied. Figures 2a and 2b shows the principles in the two steps respectively.

INSERT FIGURE 2

During the first step (CT1, Fig. 2a) the anions from the cathode compartment migrate towards the anode, in this case CO_3^{2-}. The cations in the anode compartment migrate towards the cathode, in this case Mg^{2+}. Thus, the electric field promotes transport of both these ions inside the sandstone

samples. When the concentration of Mg^{2+} and CO_3^{2-} exceed the saturation concentration of the insoluble inorganic product $MgCO_3$, precipitation will take place within the stone, and as consequence a total or partial clogging of the pores will occur.

This precipitation forms an intermediate barrier of consolidant, and a considerable increase in the electrical resistance of the stone is expected, associated to a significant decrease in the electric current flowing through the sample, as long as the potential applied remains constant between the electrodes.

At this time of treatment, three regions have developed inside the stone (Fig. 2a):

- A region close to the anode compartment rich in Mg^{2+} supplied from solution DA.
- A central region where a barrier was generated due to precipitation of the inorganic consolidant $MgCO_3$ or a hydrated form of the same compound.
- A region close to the cathode compartment rich in CO_3^{2-} supplied from solution DC.

Ending the process at this point would result in consolidation of a central region of the stone only. The surface levels, which are most susceptible to alteration processes, would remain without consolidant. For this reason, it is very important to apply the second step to reduce the pore volume also in the surface layers.

In this second step (CT2, Fig. 2b), the polarity of the electrodes is reversed and the different elements (poultices and solutions) are repositioned in their respective compartment. This new distribution of the electric field and the elements causes Mg^{2+} to migrate towards the cathode through areas of the stone enriched in CO_3^{2-} during the first step and vice versa at the cathode side. In this way, precipitation of $MgCO_3$ occurs in the more superficial volume of the stone extending the barrier, as shown in Fig. 2b.

In this study 10 samples of this stone were used, 6x6x3 cm^3 each. 5 samples per each of the two test performed were employed. One of the test consisted in the application of a single step of treatment (CT1). The other test consisted in 2 steps of the treatment (CT2).

2.4. Methods for evaluating the effectiveness

During the treatment, the potential drops over the sandstone and over a resistance (1 kΩ) connected in series were monitored. With these measurements, the resistance of the sandstone samples against the electric current flow and the intensity, which circulate within them were calculated. The analysis of these parameters is used to evaluate at which time the change from step 1 to 2 is optimal, as well as the time for ending the treatment.

At regular intervals during the treatment (every 12 hours), the pH of the solutions in M1 and M3 of both electrode compartments was measured to evaluate the buffering effects of the poultices.

After finishing the treatment, the stone samples were left to dry at room temperature, without PVC film, for one month and then the presence of the inorganic consolidant in the pores of the stones was evaluated. Stones subjected to both treatment steps (step 1 and step 2) were evaluated. For comparison a non-treated reference stone sample was included. The following techniques were used:

- The entire thickness of the sample was visualized under scanning electron microscopy (SEM) using a Philips XL-30 microscope. For this, a piece of the samples were embedded in epoxy resin, cut, polished and covered in carbon. Energy dispersive x-ray analysis (EDX) was used in order to identify the precipitates; secondary and back scattered electron modes were used.
- Also, mineralogical composition by X-ray diffraction (XRD) using a Siemens D-5000 diffractometer was obtained from the entire thickness of the sample test.
- In order to detect differences on the distribution of the precipitates along the sample, a chemical analysis was made on powder samples taken at three different depths of the test samples: near the anode, on the centre of the sample and near the cathode. In each position, three powder samples (of 1g each) were taken by drilling. Samples were prepared as pellets and were analysed by X-ray fluorescence (XRF) using a Siemens SRS-3000 spectrometer.

- Changes in the pore size distribution, by means mercury intrusion porosimetry using an AutoporeIV9500 porosimeter from Micromeritics. This determination was obtained from two areas of the samples: the area near the cathode and the area near the anode; in both areas, two samples were analysed. Using the information of this analysis, durability of the treated stone was estimated by means the DDE index explained above (Eq. 2).

Finally, to evaluate the durability of the consolidation, 2 sandstone samples per test, i.e. after 1 step and after 2 steps treatment, and 2 reference samples were completely immersed in 200 mL of ultrapure water for 8 days, always maintaining a turbulent flow with a stirring table at 150 rpm to promote the lixiviation process. Every 24 h, the quantity of Mg^{2+} released into the water was measured by ICP-OES using a Perkin Elmer Optima 4300 DV and the water was renewed. At the end of the 8 cycles the cumulative amount of Mg^{2+} released was calculated. The samples subjected to the test were also analysed by XRD, XRF and SEM-EDX; also, changes in the pore size distribution was analysed by mercury intrusion porosimetry and DDE durability index was calculated.

3. Results and Discussion

3.1. Characteristics of stone

The sandstone is composed by quartz (90%) and kaolinite (10%). Under SEM, quartz is shown as subangular grains (50-100μm) cemented by kaolinite plates (Fig 3). The elemental chemical composition (expressed as % of oxide) is the following: SiO_2 (91.51 %), Al_2O_3 (6.96 %), TiO_2 (0.44 %), K_2O (0.35 %), Fe_2O_3 (0.23 %) and P_2O_5 (0.17%); and as minor components: Na_2O (0.095 %), MgO (0.077 %), ZrO_2 (0.056 %), CaO (0.040 %), SO_3 (0.021 %), Cl (0.017%), SrO (0.012%) and Cr_2O_3 (0.008 %).

INSERT FIGURE 3

Table 1 shows the main physical properties of the stone. This stone has a water accessible porosity around 13% and a saturation degree by immersion close to 100%, which suggest a good connectivity between the pores. The difference between the accessible porosity to water and to

mercury indicates that this stone has certain pore volume not accessible to water, which would correspond to pores with access diameter lower than 0.1 μm. Capillary porosity is quite similar to water accessible porosity, suggesting that most of the pore volume of this stone lies in the range 0.1-100 μm, which corresponds to pores with pore size capillary diameter [1].

INSERT TABLE 1

Regarding the pore size distribution, this sandstone has a bimodal pore size distribution: a pore range between 0.1-10 μm (in which the 64% corresponds to pores between 1-10 μm) and a range of pores of diameter greater than 100 μm (about 5%). Only the 5% of the total porosity lies in the nanometre range. This pore size can be consulted in section 3.4 Consolidation assessment, figure 7.

The zeta potential value presented in Table 1, -24 mV, corresponds to colloidal particles obtained from the stone. Assuming that the surface of those particles is representative of the walls of the pore network in the sandstone, the fixed charge is negative, which favours the transport of cations, as it occurs for cation selective membranes [46]. Thus, the transport of Mg^{2+} will be favoured with respect to that of CO_3^{2-} in this stone.

3.2. Current intensity and resistance

Figure 4 shows the average measurements (n= 5 samples per test) of resistance and the intensity of electrical current registered during the two steps of the treatments.

INSERT FIGURE 4

In the first 5 days of each treatment, the resistance is low and the current intensity relatively high, though decreasing. After this time, the resistance increased at the same time as the current intensity decreased, which indicates that the ions find a greater difficulty in their transport towards the electrode of opposite polarity. This can be related to a possible precipitation of $MgCO_3$ in the pores of the sandstone, as both pore clogging and precipitation (and thus loss of free ions) will result in an increased resistivity, which is in accordance with [38]. After 17 days of treatment, the

resistance increased from 0.58 kΩ to about 20 kΩ, while the current intensity decreased from 6 mA to 1mA. The asymmetry between both evolutions is due to the 1 kΩ series resistor that initially limits the current flow due to the low resistance of the sandstone samples.

At the 17th day, the treatment was stopped on the samples subjected to step 1 (CT1), whereas it was maintained for 7 more days for the samples subjected to step 2 (CT2). During this period, the resistance reached values close to 60 kΩ and the current intensity fell down close to 0 mA, suggesting that a precipitation of a compound into the pores took place. At this moment, step 2 was started in these samples, by reversing the polarity of the electrodes and consequently changing the solutions and poultices. At the beginning of the step 2, a sharp fall on the resistance and a sudden rise on the current intensity took place, but after this, and as occurred during step 1, intensity began to drop and resistance began to rise, suggesting again that a possible precipitation into the pores of the rock took place.

3.3. pH changes

The pH measurements showed that extreme pH values were reached in the solution in section M1. It reached close to 2 at the anode and 13 at the cathode, which is in accordance with previous reports [23-24]. The buffering poultice in section M2 worked as planned, as pH of the solutions in M3 remained at the same level as the initial pH.

In addition to hindering extreme pH environments and subsequent damage of the stone, the buffer poultice probably increased the efficacy of the precipitation process, as the transport of the more mobile ions H^+ and OH^-, are hindered. The transport of these ions into the stone would reduce the transport number (parameter that relates the charge transported by one ion with respect to the total charge passed through the stone) of the ions of interest as discussed for other electrokinetic treatments in [47-49].

3.4. Consolidation assessment

In Figure 5, SEM micrographs of the stone subjected to step 1 (CT1) and step 2 (CT2) are shown. In the SEM images of the reference sandstone (Fig. 3), the pores are clearly visible both in the skeleton and among the kaolinite packages. In CT1 samples, pores are filled with a crystalline precipitate rich in Mg and C, suggesting that the precipitation of magnesium carbonate took place (similar results to those reported in section Durability of the consolidation, figure 9). These precipitates fill the larger pores but also those the smallest between kaolinite plates. SEM visualization allowed confirming that the amount of these precipitates is higher from the centre of the test samples towards the cathode. On the contrary, in CT2 samples (Fig 5), the precipitates fill the pores of the stone along the entire thickness of the test sample, i.e. superficial and internal pores.

INSERT FIGURE 5

X- ray diffraction confirmed that the precipitates correspond to nesquehonite $MgCO_3 \cdot 3(H_2O)$; a hydrated form of magnesium carbonate. This result is in accordance the radial-shaped habit of the crystals visualized under SEM.

Figure 6 shows the average percentages of MgO obtained by XRF in the treated and untreated samples, in three different areas of the test samples (near the anode, in the middle and near the cathode). Before the lixiviation process, in the untreated stone the content of MgO is very low (0.071%). In CT1 samples enrichment on MgO is produced in all the areas sampled, especially at the cathodic side. This fact could be related to the different mobility of the ions entering the rock: Mg^{2+} has a greater mobility than CO_3^{2-} due to the charge of the pore walls; so, this favours the precipitation of the hydrate magnesium carbonate in the vicinity of the cathode, forming a first barrier near this area. In CT2 samples an increase in MgO concentration with respect to the CT1 samples was observed at all sampled levels, especially in the zones near the anode and in the middle zone.

INSERT FIGURE 6

Figure 7 show the average pore size distribution of the reference sample and the treated samples CT1 and CT2 taken near the anode and near the cathode. Table 2 shows the physical properties (tortuosity and accessible porosity to mercury) and durability factor DDE for these sandstones.

INSERT FIGURE 7

After the step 1, a reduction in the pore volume of the sandstone samples is obtained (see Fig. 8a, continuous line, and Table 2): in the anode area, the accessible porosity decreased from 17.4% to 16.2% whereas in cathode area, the accessible porosity decreased to 16%. This slight difference between the Hg accessible porosity between the anode and cathode zones suggest that the consolidation during step 1 took place mainly in the area closest to the cathode. This fact could be related with the comments above (the negative surface charge of the pore network).

In CT2 samples (see Fig. 7b, continuous line, and Table 2) the reduction on Hg accessible porosity achieved at the cathode side were higher (13.9%) than that obtained for CT1 samples (16%) while at the anode it remains unchanged (16.2%).

Analysing the pore size distributions of CT1 samples comparatively to untreated stone (Fig 7a), it can be seen that, in the cathode area, a reduction in the volume of pores with an access diameter greater than about 5 μm and especially in the volume of pores with an access diameter higher than 100 μm occurred. There was also a pore volume displacement between 5 and 1 μm, with a slight enrichment in the pore range with an access diameter lower than 5 μm. These increases may be due to the partial filling of wider pores, which causes decrease in their access size. In the anode side, the decrease in pore volume was mainly on pores with access diameter between approximately 5-10 μm. In this area no decrease in pores of wider size was registered. However, an increase in the pore volume of access between 1-4 μm was observed, probably due to the partial filling of some wider pores.

The changes of the pore size distribution on CT2 samples (Fig 7b) are similar to those achieved on CT1 samples. At the cathode side, a larger reduction in the pore volume higher than 5 μm and a slight increase in the pore volume below 5 μm are shown. In the anode side, the pore size

decrease affected mainly the pore range with access diameter between 5-50 μm, not affecting the pores wider than 50 μm, and causing an increase in the pore volume lower than 5 μm.

INSERT TABLE 2

The porosity reductions observed would be due to the precipitation of the hydrated magnesium carbonate. Also, this reduction took placed mainly in the wider pores. This fact is in accordance with previous works [3, 24, 49]: the work reported in ref. [3] focuses on soluble salts and reports that salts crystallization begins in the wider pores and then progresses into the smaller pores. In [24], work focused on electro-desalination, a decrease in the pore volume with an access diameter greater than 50 μm and a slight increase in the pore volume with an access diameter between 0.1 and 10 μm was also registered. In [49], where migration of silicate ions was proposed in order to produce calcium silicate hydrate (C-S-H) gel in the pores of concrete, similar results were achieved.

Tortuosity (Table 2) decreased after the treatments; being the tortuosity of pore system of CT2 samples lower than that of CT1 samples. This finding is supported by [25] and indicates that the total or partial pore blocking must occur in the percolation pores of the stone, which initially has a higher tortuosity. The DDE index decreased after the treatment, especially in the cathode area, indicating that the treatment enhance the durability of the stone. The increase in durability was slightly higher after the application of the two steps (CT2).

All of these data confirm that the reversion of the polarity of the electrodes favour an increase of the consolidated area, beyond the cathodic area.

3.5. Durability of the consolidation

As explained on material and methods section, a lixiviation test was performed in order to known the resistance of the precipitate to water lixiviation.

In Figure 7 and Table 2, pore size distribution and porosity parameters of the consolidated CT1 and CT2 samples subjected to the lixiviation test is shown and the comparison with the same

samples not subjected to this test can be made. After the lixiviation process, the porosity of the CT1 samples increased (Table 2), reaching values similar to those for the reference stone, especially in the anode side. The porosity of CT2 samples subjected to the lixiviation test also showed an increase but not as high as occurred in CT1 samples: the porosity was increased from 16.2% to 16.9% at the anode and from 13.9% to 15.0% at the cathode. In Figure 7, it can be seen that the increase on porosity is due to an increase on pores with an access diameter higher than 5 μm in the anode side and to an increase of the pores with an access diameter greater than 8 μm in the cathode side.

After the lixiviation process, an increase in the tortuosity of the porous network is obtained, reaching values of tortuosity higher than that of the reference stone, especially in CT1 samples. This can be related to the partial dissolution of the magnesium compound in some of the pores in the stone, leaving them partially filled. In this way, the ions penetrating the material will find a greater difficulty in transport through the interior of the pore network. The DDE index obtained after the lixiviation test increased to similar values of the reference stone, especially in the anode side.

The increases on the porosity after the lixiviation test can be related to the solubilisation of the hydrated magnesium carbonate during the test, which is verified by ICP OES and XRF analyses. In Figure 8, the kinetic release of Mg^{2+} from untreated samples, CT1 and CT2 samples during the lixiviation test is shown. In general it can be seen that 1) the amount of Mg^{2+} released from the treated samples was much higher than the Mg^{2+} released from the reference; 2) the kinetic of release is similar in the three kind of samples: during the first day, a quick liberation of Mg took place; from this moment, the release of Mg became constant. These release dynamics indicate that the quantity of magnesium released is very low after 4 days. The amount of Mg released is higher in CT1 samples than in CT2 samples; this could be related to 1) the presence on CT1 samples of a higher amount of free Mg^{2+} ions or 2) The lower porosity of CT2 samples (Table 2), which reduces the amount of water absorbed during the lixiviation test.

INSERT FIGURE 8

Figure 6 depicts the Mg content (expressed as % MgO) of samples taken at three different areas of the samples (near the cathode, on the middle of the sample and near the anode) before and after the lixiviation test. In CT1 samples, a notable reduction in MgO content is produced after the lixiviation test, especially in the cathode zone. In the samples CT2, a slight increase of MgO is found in the area near the anode, which could be due to the diffusion of dissolved Mg^{2+} towards this surface during the drying process and to the subsequent precipitation of part of the dissolved Mg^{2+} in this area. In the middle area and in the area near the cathode, a slight Mg^{2+} loss is produced but the Mg remained into the rock is higher than that on the same areas of CT1 samples. This suggest, in accordance with data from Figure 8, that the magnesium precipitate formed in CT2 samples is more resistance to solubilisation than that formed in CT1 samples.

Figure 9 shows the SEM image of a CT2 sample after the lixiviation process. It is seen that the inorganic consolidant formed inside the pores remains. The EDX analysis performed shows that the pore-filling compound is mainly composed of magnesium, an element that is barely present in the untreated sandstone, and carbon, which again confirms that the precipitated product is a magnesium carbonate compound with a radial-shaped crystallization habit. X-ray diffraction confirmed again that the precipitate correspond to nesquehonite $MgCO_3 \bullet 3(H_2O)$.

INSERT FIGURE 9

4. Conclusions

The main conclusion drawn from this study is that electrokinetic consolidation, following the proposed procedure, allows to consolidate sandstone throughout the entire sample section by precipitating $MgCO_3 \cdot 3(H_2O)$ as consolidant in the pores. In consequence this treatment allows increasing their durability against the action of external alteration agents.

A new designed buffering system prevents the treated sandstone to be exposed to extreme pH values resulting from electrolysis at the electrodes. The buffering system also serves as source for the ions electromigrating into the sandstone to block the pores and consolidate it.

The treatment procedure has two steps, between which the current was reversed, but the electrode units were kept. The current reversal ensured a better consolidation in a larger part of the sandstone. The treatment allows to consolidate, during the first step, the pores just to a deeper depth; the precipitation of the compound takes place in this step in areas closer to the cathode, due to the zeta potential of the material. In the second step, the consolidation of the rest of the pores, through which the current flows, occurs, i.e. from areas adjacent to the first consolidated area to the most superficial pores.

The stability of the consolidant was tested by accelerated lixiviation process. The results indicate that despite a rapid release of magnesium during the first day, the release of magnesium stagnates after the fourth day, remaining a high amount of precipitate in the stones. In consequence this treatment improves durability of the current consolidation treatments.

Acknowledgments. J. Feijoo work was supported by the Ministerio de Educación, Cultura y Deporte, Spanish Government, through a FPU grant.

References

[1] Winkler, E.M. (1997). Stone in Architecture: Properties, Durability, 3rd ed. Springer-Verlag, Berlin, 309 p.

[2] Benavente, D., Linares-Fernández, L., Cultrone, G., & Sebastián, E. (2007). Influence of Microstructure on the Resistance to Salt Crystallisation Damage in Brick. *Materials and Structures*, *39*, 105–113. doi:10.1617/s11527-005-9037-0

[3] La Iglesia, a., González, V., López-Acevedo, V., & Viedma, C. (1997). Salt crystallization in porous construction materials I Estimation of crystallization pressure. *Journal of Crystal Growth*, *177*, 111–118. doi:10.1016/S0022-0248(96)01072-X

[4] Bubeck, a., Walker, R. J., Healy, D., Dobbs, M., & Holwell, D. a. (2017). Pore geometry as a control on rock strength. Earth and Planetary Science Letters, 457, 38–48. doi:10.1016/j.epsl.2016.09.050

[5] Jefferson, D. P. (1993). Building Stone - The Geological Dimension. *Quarterly Journal of Engineering Geology*, *26*, 305–319. doi:10.1144/GSL.QJEGH.1993.026.004.06

[6] Esbert, R. M., Ordaz, J., Alonso, F. J., & Montoro, M. (1997). Manual de diagnosis y tratamiento de materiales pétreos y cerámicos. *Manuals de diagnosi* (Vol. 5, p. 140). ISBN: 84-87104-29-0.

[7] Gauri, K.L., Bandyopahyay, J.K. (1999). Carbonate stone: chemical behavior, durability and conservation. New York, John Wiley & Sons, 284 p.

[8] Hall, Christopher; Hoff, W. D. (2009). *Water Transport in Brick, Stone and Concrete*. *Cement, Concrete and Aggregates* (Vol. 25, p. 362). doi:10.1520/CCA10518J

[9] Takarli, M.; Prince, W.; Siddique, R. (2008). Damage in granite under heating/cooling cycles and water freeze–thaw condition International Journal of Rock Mechanics & Mining Sciences 45, 1164–1175.

[10] Ruedrich, J., Kirchner, D., & Siegesmund, S. (2011). Physical weathering of building stones induced by freeze-thaw action: A laboratory long-term study. *Environmental Earth Sciences*, *63*, 1573–1586. doi:10.1007/s12665-010-0826-6

[11] Warscheid, T., & Braams, J. (2000). Biodeterioration of stone: A review. *International Biodeterioration and Biodegradation*, 46, 343-368. doi:10.1016/S0964-8305(00)00109-8

[12] Feijoo, J., Matyščák, O., Ottosen, L. M., Rivas, T., & Nóvoa, X. R. (2017). Electrokinetic desalination of protruded areas of stone avoiding the direct contact with electrodes. *Materials and Structures/Materiaux et Constructions*, *50*. doi:10.1617/s11527-016-0946-x

[13] Pel, L., Huinink, H., & Kopinga, K. (2003). Salt transport and crystallization in porous building materials. In *Magnetic Resonance Imaging* (Vol. 21, pp. 317–320). doi:10.1016/S0730-725X(03)00161-9

[14] Cárdenes, V., Mateos, F. J., & Fernández-Lorenzo, S. (2014). Analysis of the correlations between freeze-thaw and salt crystallization tests. *Environmental Earth Sciences*, *71*, 1123–1134. doi:10.1007/s12665-013-2516-7

[15] Franzoni, E. (2014). Rising damp removal from historical masonries: A still open challenge. *Construction and Building Materials, 54,* 123-136. doi:10.1016/j.conbuildmat.2013.12.054

[16] Charola, A.E & Herodotus (2000). Salts in the deterioration of porous materials: an overview: *Journal of American Institute for Conservation,* 39, 327-343.

[17] Unruh, J. (2001). A revised endpoint for ceramics desalination at the archaeological site of Gordion, Turkey. *Studies in Conservation*, *46*, 81–92. doi:10.2307/1506839

[18] Lubelli, B., & van Hees, R. P. J. (2010). Desalination of masonry structures: Fine tuning of pore size distribution of poultices to substrate properties. *Journal of Cultural Heritage*, *11*, 10–18. doi:10.1016/j.culher.2009.03.005

[19] Vergès-Belmin, V., & Siedel, H. (2005). Desalination of Masonries and Monumental Sculptures by Poulticing: A Review. *Restoration of Buildings and Monuments. 11*, 391–408. doi:10.1515/rbm-2005-6000

[20] Teresa Rivas, Jorge Feijoo, Iván de Rosario & Javier Taboada (2017): Use of Ferrocyanides on Granite Desalination by Immersion and Poultice-Based Methods, *International Journal of Architectural Heritage*, doi:10.1080/15583058.2016.1277282

[21] Ottosen, L. M., & Rörig-Dalgård, I. (2007). Electrokinetic removal of $Ca(NO_3)_2$ from bricks to avoid salt-induced decay. *Electrochimica Acta*, *52*, 3454–3463. doi:10.1016/j.electacta.2006.03.118

[22] Ottosen, L.M. and Rörig-Dalgaard, I. (2009), Desalination of a brick by application of an electric DC field. *Materials and Structures*, *42,* 961-971. doi:10.1617/s11527-008-9435-1

[23] Feijoo, J., Nóvoa, X. R., Rivas, T., Mosquera, M. J., Taboada, J., Montojo, C., & Carrera, F. (2013). Granite desalination using electromigration. Influence of type of granite and saline contaminant. *Journal of Cultural Heritage*, *14*, 365–376. doi:10.1016/j.culher.2012.09.004

[24] Feijoo, J., Ottosen, L. M., & Pozo-Antonio, J. S. (2015). Influence of the properties of granite and sandstone in the desalination process by electrokinetic technique. *Electrochimica Acta, 181,* 280–287. doi:10.1016/j.electacta.2015.06.006

[25] Doehne, E. and Price C.A. (2010). Stone Conservation. An Overview of Current Research. Published by the Getty Conservation Institute. ISBN 978-1-60606-046-9, 158 p.

[26] Scherer, G. W., & Wheeler, G. S. (2009). Silicate consolidants for stone. *Key Engineering Materials*, *391*, 1–25. doi:10.1016/j.culher.2006.10.002

[27] Wheeler, G. (2005). *Alkoxysilanes and the Consolidation of Stone*. *Journal of the American Institute for Conservation, 46*, 189–191. doi:10.1007/s13398-014-0173-7.2

[28] De Rosario, I., Elhaddad, F., Pan, A., Benavides, R., Rivas, T., & Mosquera, M. J. (2015). Effectiveness of a novel consolidant on granite: Laboratory and in situ results. *Construction and Building Materials*, *76*, 140–149. doi:10.1016/j.conbuildmat.2014.11.055

[29] Price, C., Ross, K., & White, G. (1988). A further appraisal of the “lime technique” for limestone consolidation, using a radioactive tracer. *Studies in Conservation*, *33*, 178–186. doi:10.2307/1506313

[30] Sassoni, E.; Naidu, S.; Scherer, G.W. (2011). The use of hydroxyapatite as a new inorganic consolidant for damaged carbonate stones. *Journal of Cultural Heritage, 12,* 346-355.

[31] Siegesmund, S. and Snethlage, R. (2011). Stone in Architecture: Properties, Durability. Springer. 4th ed. 2011 Edition. ISBN-13: 978-3642144745. 552 p.

[32] Slavíková, M.; Krejcí, F.; Žemlička, J.; Pech, M.; Kotlík, P.; Jakubek, J. (2012). X-ray radiography and tomography for monitoring the penetration depth of consolidants in Opuka – the building stone of Prague monuments. *Journal of Cultural Heritage, 13*, 357–364

[33] Slavíková, M.; Krejcí, F.; Kotlík, P.; Jakubek, J.; Tomandl, I.; Vacík, J. (2014). Neutron and high-contrast X-ray micro-radiography as complementary tools for monitoring organosilicon consolidants in natural building stones. *Nuclear Instruments and Methods in Physics Research B, 338,* 42–47.

[34] Chiantore, O., & Lazzari, M. (2001). Photo-oxidative stability of paraloid acrylic protective polymers. *Polymer*, *42*, 17–27. doi:10.1016/S0032-3861(00)00327-X

[35] Varas-Muriel, M. J., Pérez-Monserrat, E. M., Vázquez-Calvo, C., & Fort, R. (2015). Effect of conservation treatments on heritage stone. Characterisation of decay processes in a case study. *Construction and Building Materials*, *95*, 611–622. doi:10.1016/j.conbuildmat.2015.07.087

[36] Balliana, E., Ricci, G., Pesce, C., & Zendri, E. (2016). Assessing the value of green conservation for cultural heritage: positive critical aspects of alreafy available methodologies. *International Journal of Conservation Science*, 7, 185–202.

[37] Meloni, P.; Manca, F.; Carcangiu, G. (2013). Marble protection: An inorganic electrokinetic approach. *Applied Surface Science, 273, 377-385.*

[38] Bernabeu, A., Expósito, E., Montiel, V., Ordóñez, S., & Aldaz, A. (2001). A new electrochemical method for consolidation of porous rocks. *Electrochemistry Communications*, *3*, 122–127. doi:10.1016/S1388-2481(01)00117-5

[39] Amoros J. L., Beltran, V., Escardino, A., Orts, Ma. J. (1992). Permeabilidad al aire de soportes cocidos de pavimento cerámico II. Relación entre el coeficiente de permeabilidad al aire y las propiedades características de la estructura porosa del sólido. Bol. Soc. Esp. Ceram. Vidr. 31 3, 207-212.

[40] Ordonez, S., Fort, R., & Garcia del Cura, M. A. (1997). Pore size distribution and the durability of a porous limestone. *Quarterly Journal of Engineering Geology and Hydrogeology*, *30*, 221–230. doi:10.1144/GSL.QJEG.1997.030.P3.04

[41] Bell, F.G. (1993). Durability of carbonate rock as building stone with comments on its preservation. *Environmental Geology, 21*, 187-200. doi:10.1007/BF00775905

[42] Rossi-Manaresi, R.; Tucci, A. (1989). Pore structure and salt crystallization: 'salt decay' of Agrigento biocalcarenite and 'case bardenin' in sandstone. Proceedings 1st International Symposium, Bari, 'The Conservation of monuments in the Mediterranean Basin': 97-100.

[43] RILEM (Réunion Internationale des Laboratoires d'Essais et de Recherche sur les Matériaux et les Constructions) 1980. Commission 25 PEM. Protection et Erosion des Monuments. Recommandations provisoires. Essais recommandés pour mesurer l'altération des pierres et évaluer l'efficacité des méthodes de traitement. Test No. II. 1: Open porosity and Test II. 2: Bulk and real densities.

[44] ICR-CNR- Instituto Centrale do restauro- Commisione Normal. (1985). Doc. NORMAL 11/85. Assorbimento d'acqua per capilaritá. Coefficiente di assorbimento capillare.

[45] ICR-CNR-Instituto Centrale do Restauro-Commisione Normal. (1981). Doc. NORMAL 7/81. Assorbimento d'acqua per immersione totale. Capacitá di imbibizione.

[46] Tanaka, Y. (2015). Ion exchange membranes fundamentals and applications, 2nd ed., Elsevier Science. ISBN:9780444633194.

[47] Castellote, M.; Andrade, C.; Alonso, C. (2000). Electrochemical removal of chlorides Modelling of the extraction, resulting profiles and determination of the efficient time of treatment. *Cement and Concrete Research, 30,* 615-621.

[48] Ottosen, L. M., Ferreira, C. M. D., & Christensen, I. V. (2010). Electrokinetic desalination of glazed ceramic tiles. In *Journal of Applied Electrochemistry, 40,* 1161–1171. doi:10.1007/s10800-010-0086-x

[49] Shan, H., Xu, J., Wang, Z., Jiang, L., & Xu, N. (2016). Electrochemical chloride removal in reinforced concrete structures: Improvement of effectiveness by simultaneous migration of silicate ion. *Construction and Building Materials*, *127*, 344–352. doi:10.1016/j.conbuildmat.2016.09.137

FIGURE CAPTIONS

Figure 1. Schematic diagram of the different parts and elements which forming the electrokinetic setup made it for the consolidation treatment.

Figure 2. Schematic diagram of the procedure used for consolidate the stone composed of two phases (first step a), samples called CT1; second step b), samples called CT2).

Figure 3. SEM photograph of the yellow sandstone untreated (Reference).

Figure 4. Average of measurements (n=5) of resistance in kΩ (a) and current intensity in mA (b) recorded during the consolidation treatment with 1 step (CT1) and with 2 steps (CT2).

Figure 5. SEM photographs of the yellow sandstone treated with 1 step (CT1) and 2 steps (CT2).

Figure 6. Average content of MgO in percentage at different levels in samples treated with 1 step (CT1), with 2 steps (CT2) and untreated (Reference), before and after the lixiviation process.

Figure 7. Average pore size distribution (n=2) of the reference samples and CT1 samples consolidated under only 1 step (a) and their subsequent lixiviation (dashed line) and the CT2 samples consolidated under 2 steps (b) and their subsequent lixiviation (dashed line), in the surface close to the anode and the surface close to the cathode.

Figure 8. Average concentration (n=2) of magnesium (in mg/L) released during the leaching process in water, in samples treated with 1 step (CT1), with 2 steps (CT2) and untreated (Reference).

Figure 9. SEM photograph and EDX analyses of the yellow sandstone treated with 2 steps and lixiviate. Also the elemental maps of Mg, C, Si and Al are shown.

Figure 1

Click here to download colour figure Figure 1.JPG

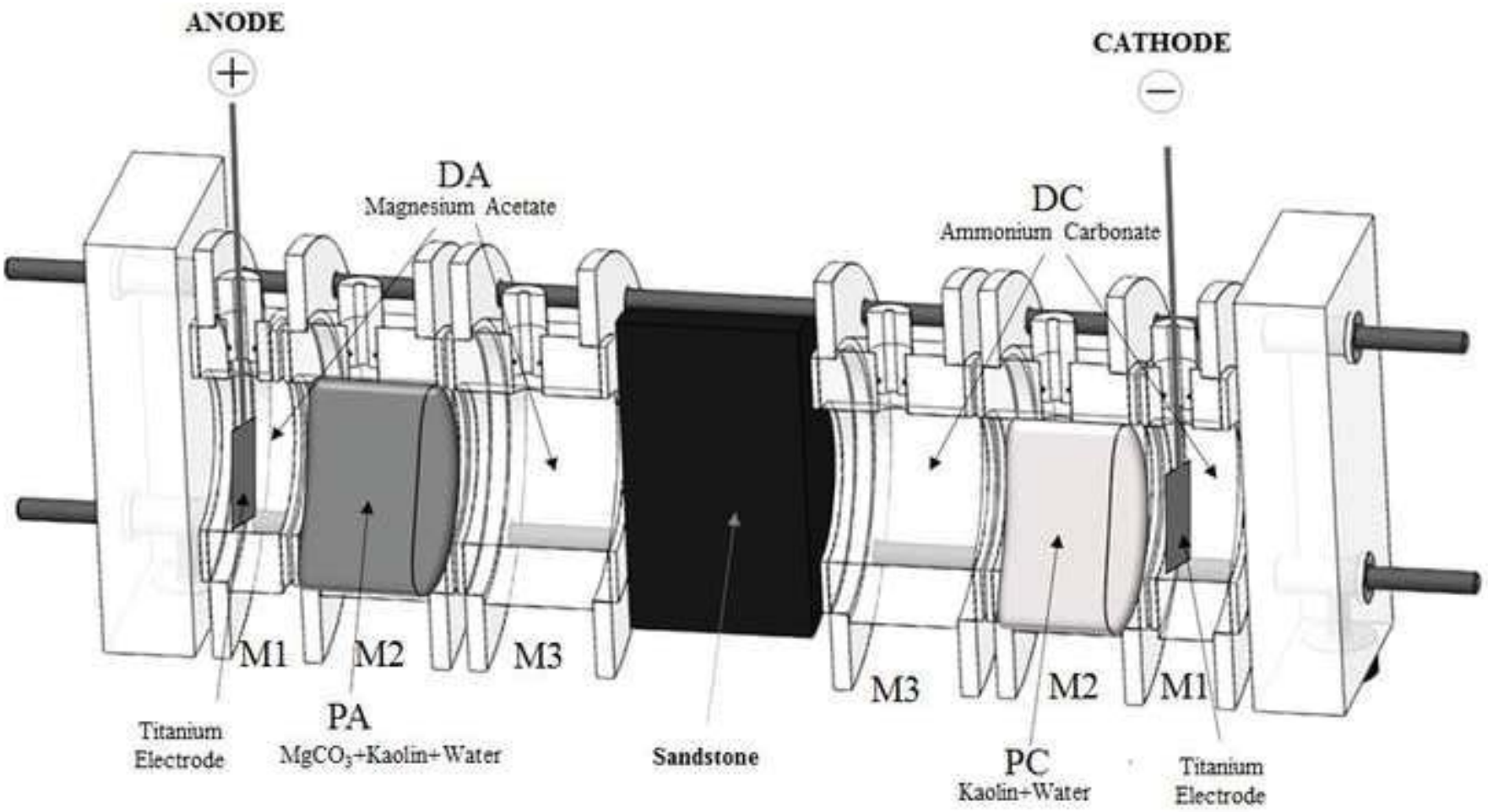

Figure 2

Click here to download colour figure Figure 2.jpg

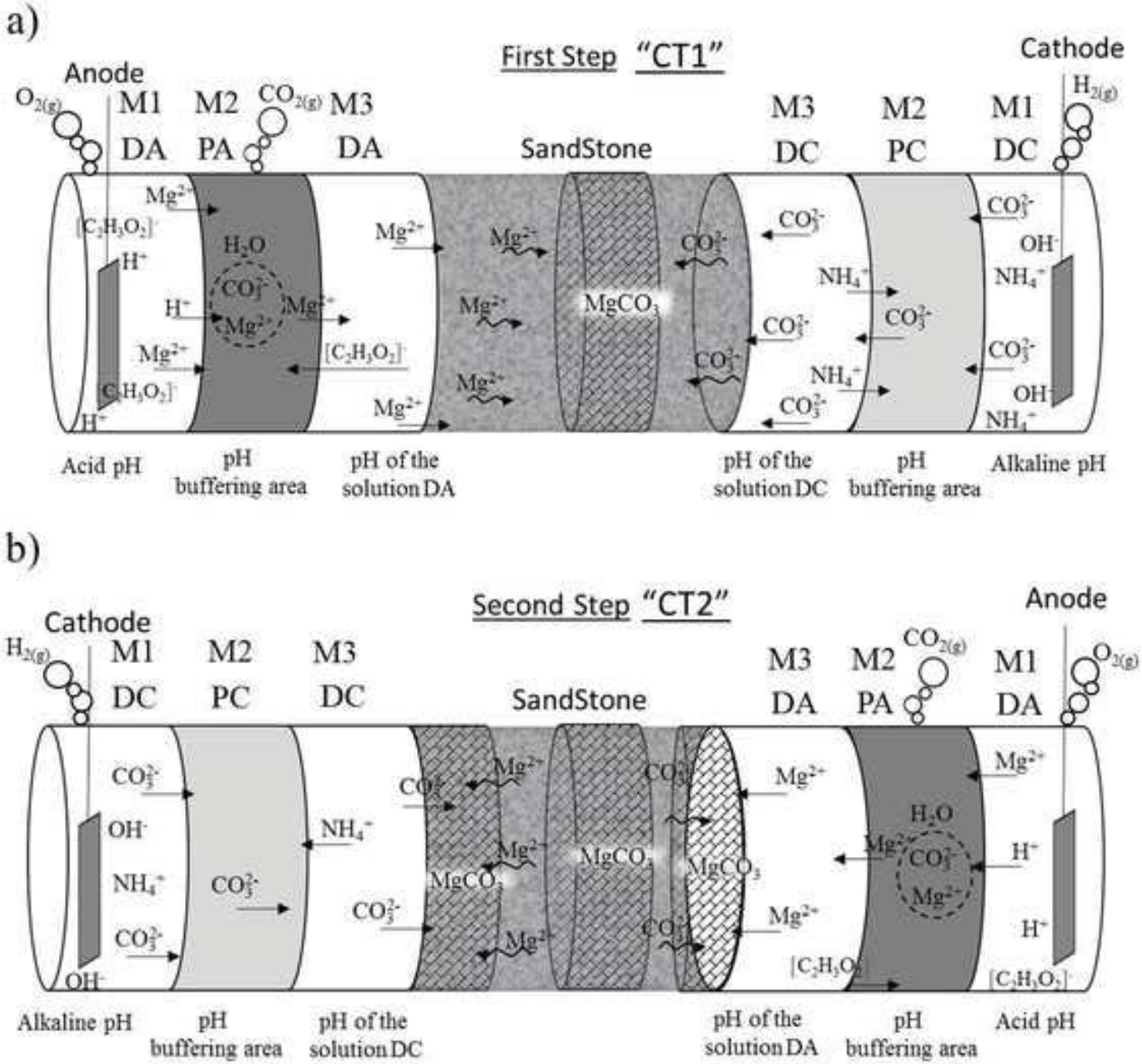

Figure 3

Click here to download colour figure Figure 3.jpg

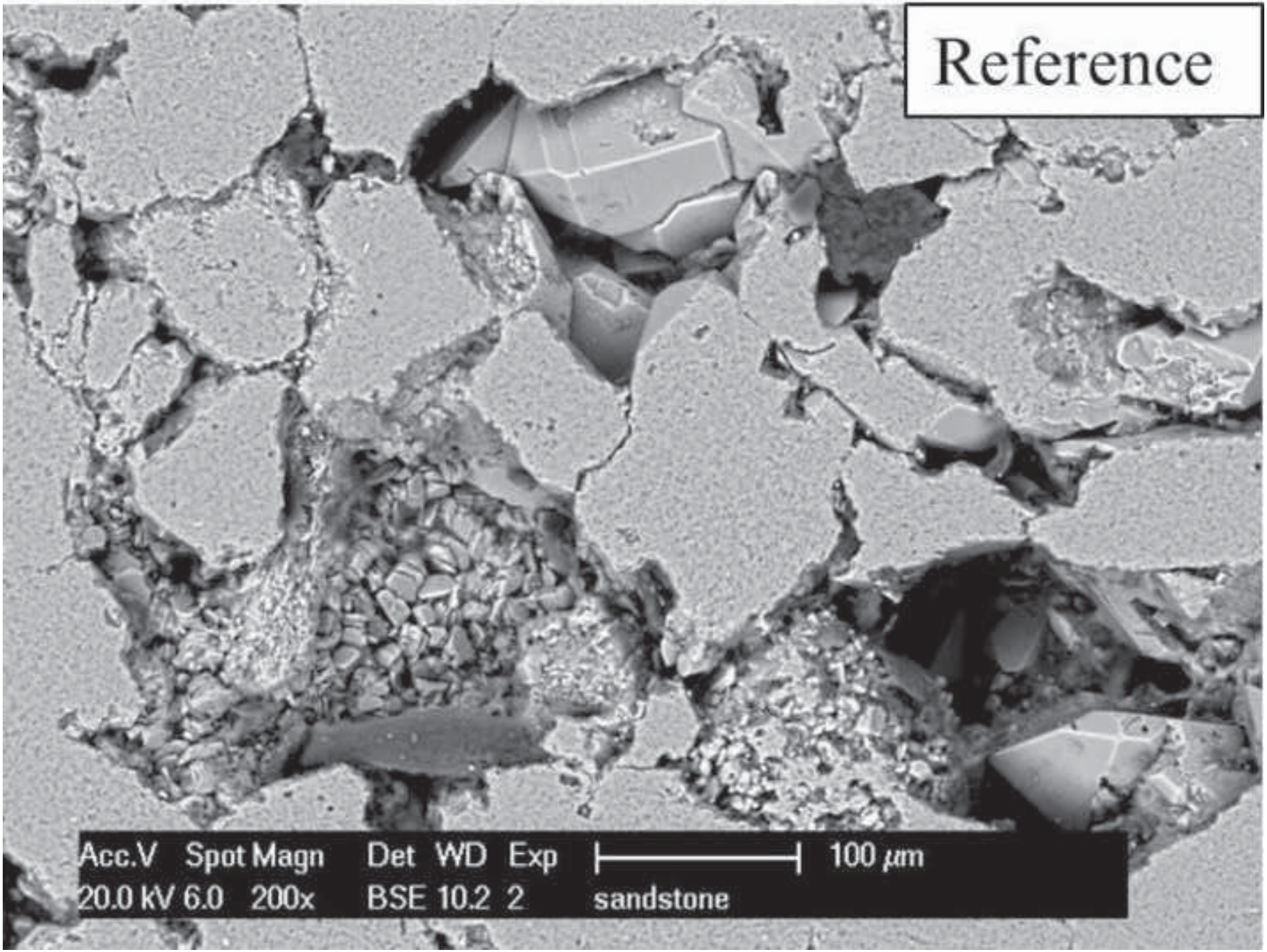

Figure 4

Click here to download colour figure Figure 4.jpg

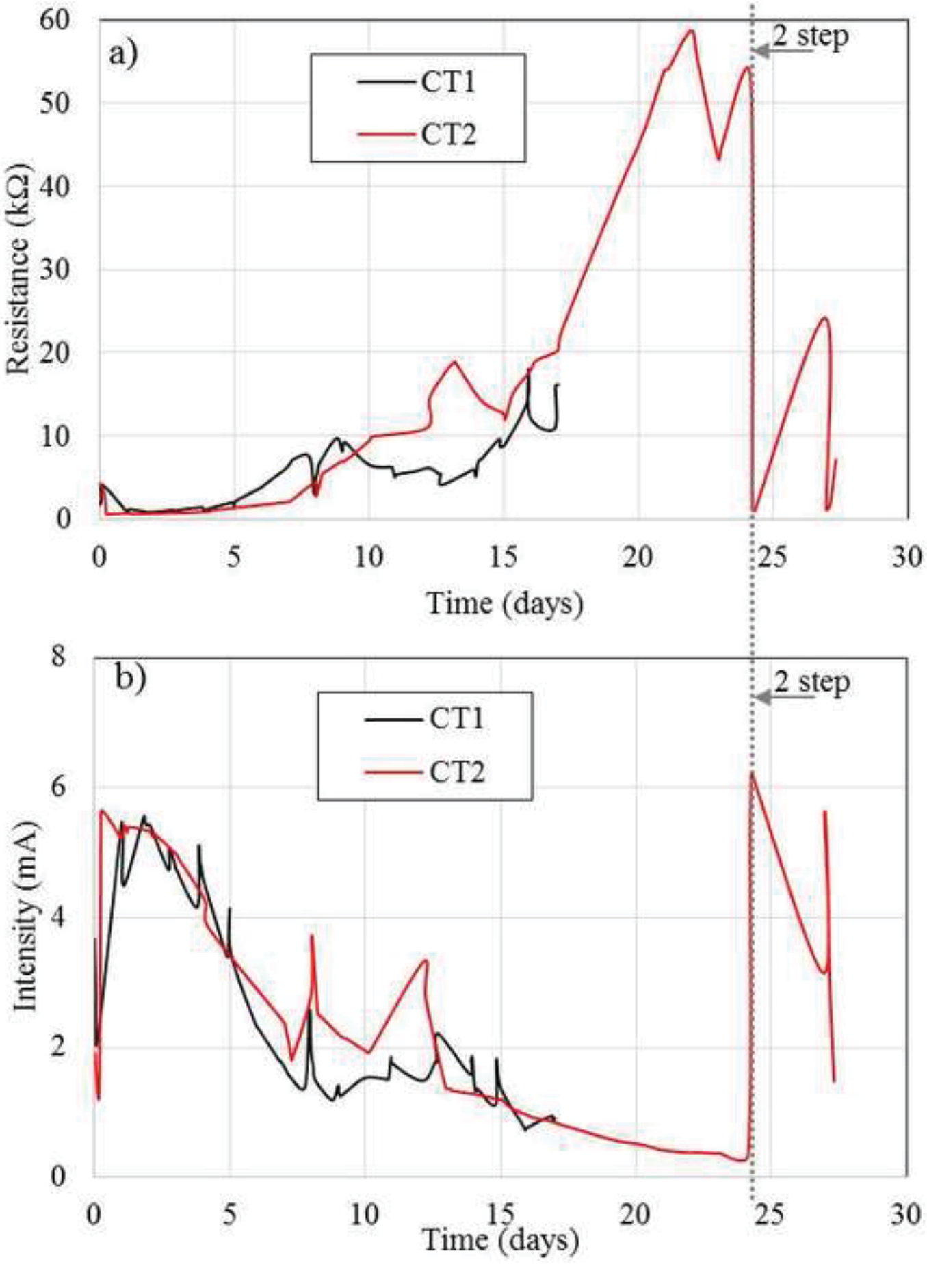

Figure 5

Click here to download colour figure Figure 5.jpg

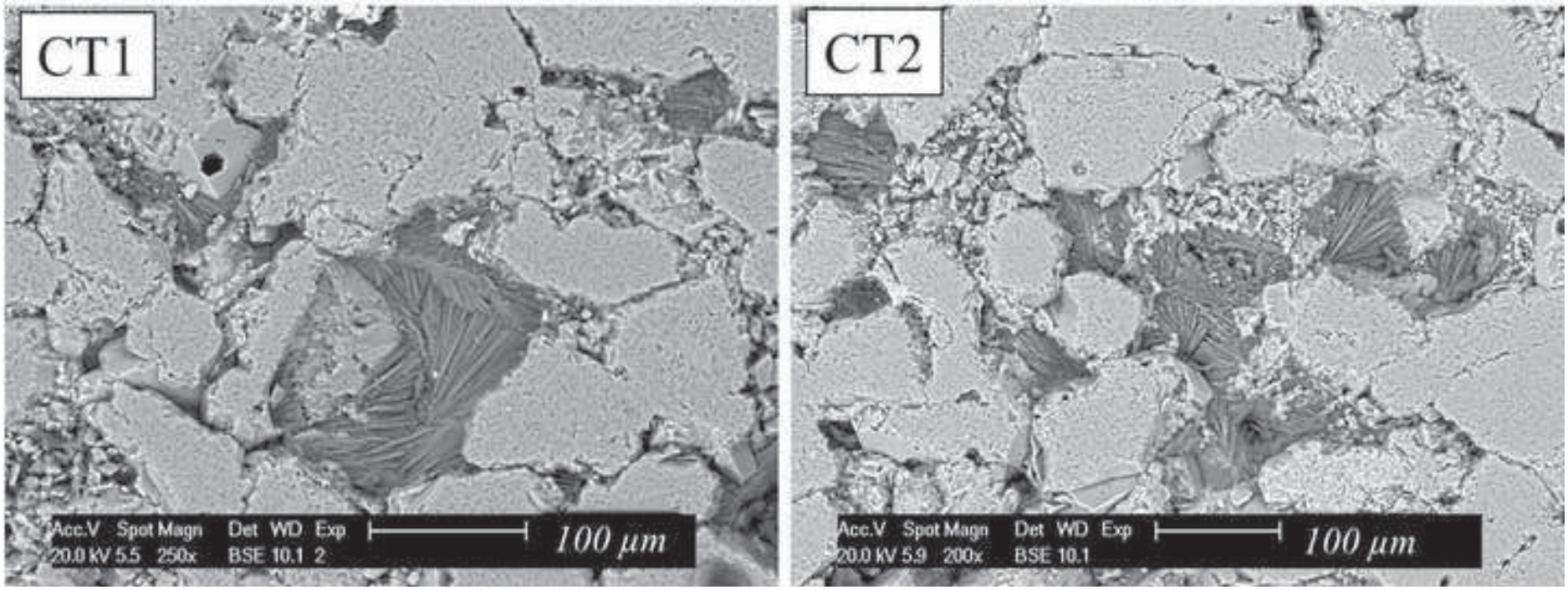

Figure 6

Click here to download colour figure Figure 6.JPG

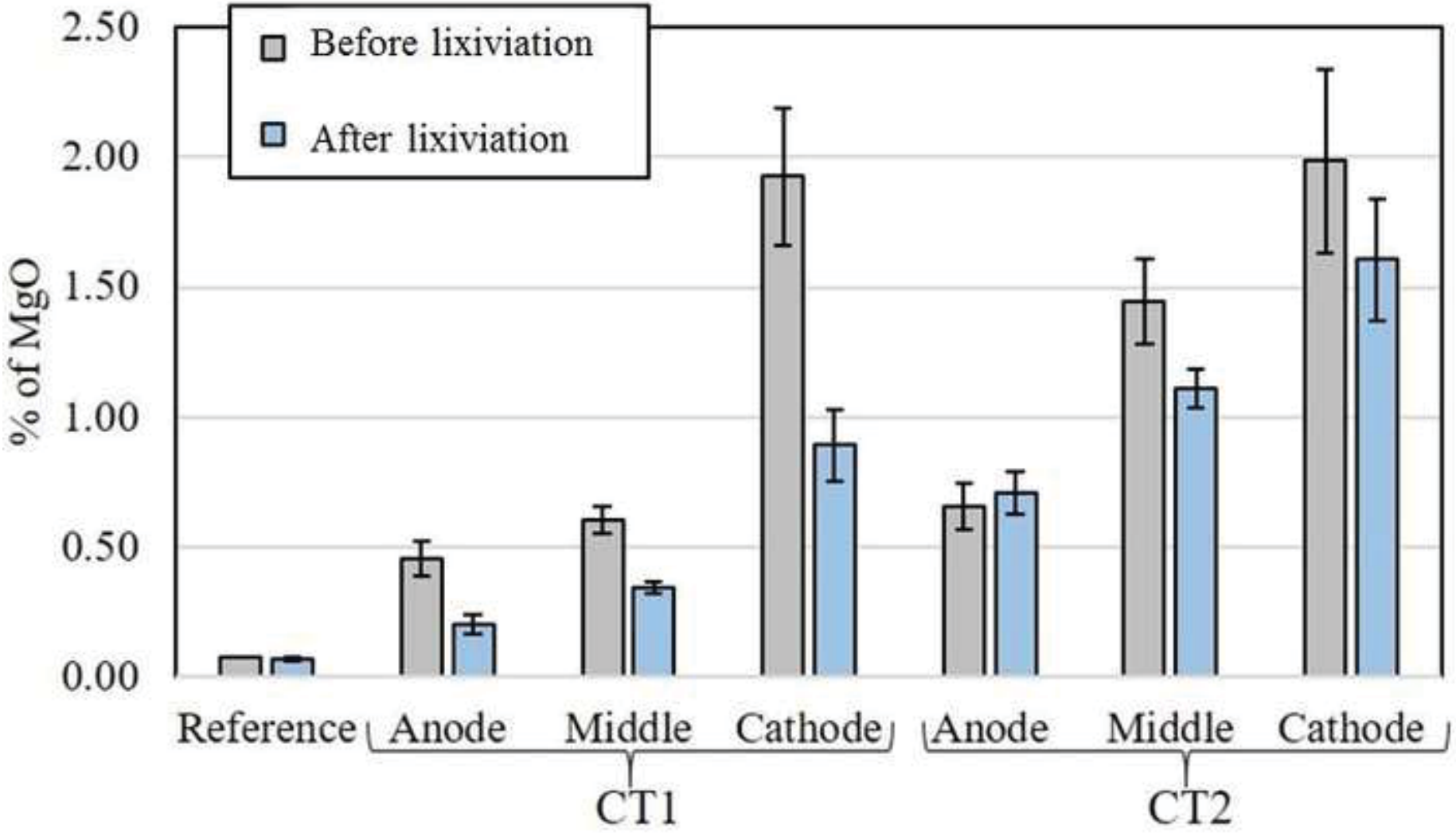

Figure 7

Click here to download colour figure Figure 7.jpg

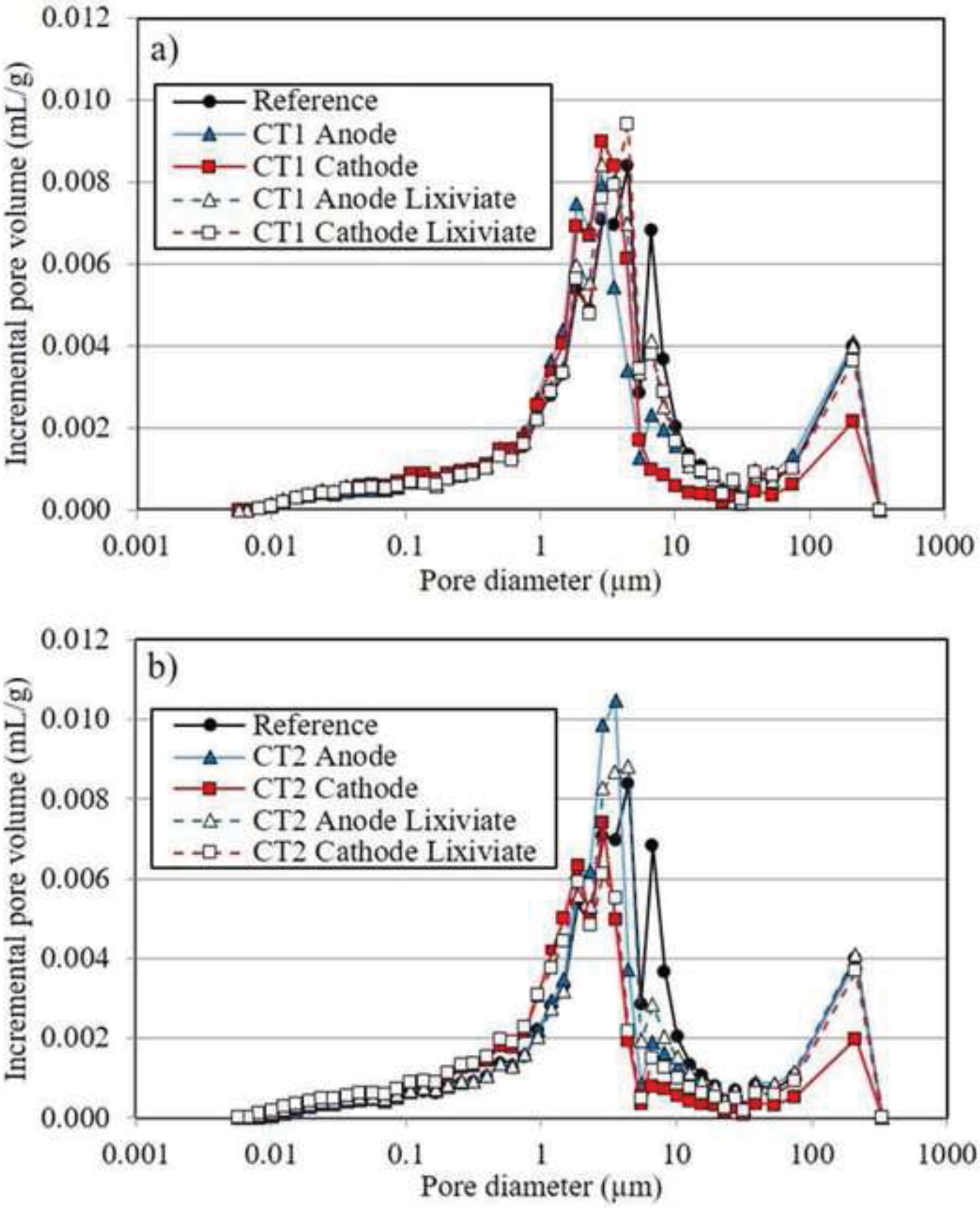

Figure 8

Click here to download colour figure Figure 8.jpg

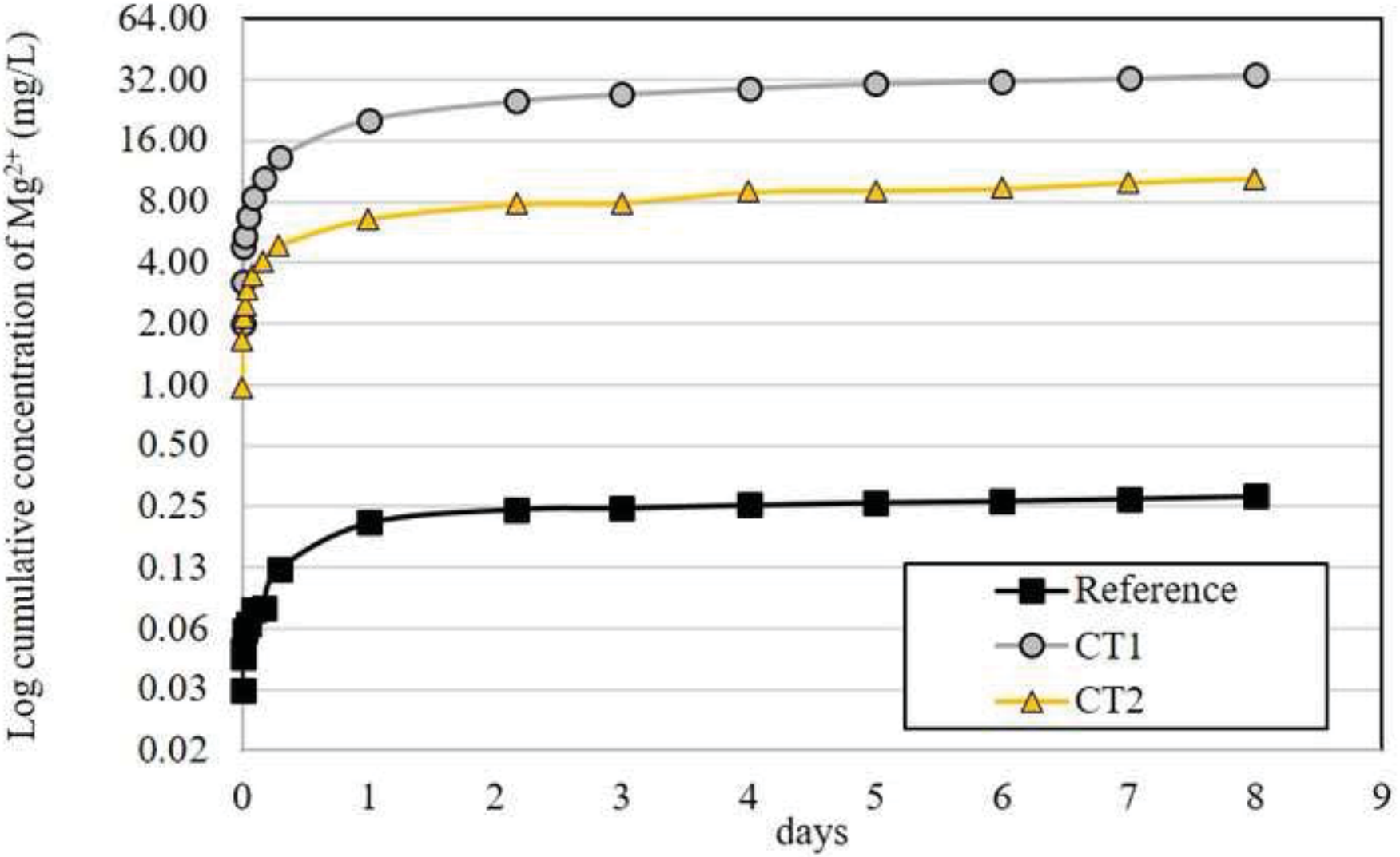

Figure 9

Click here to download colour figure Figure 9.jpg

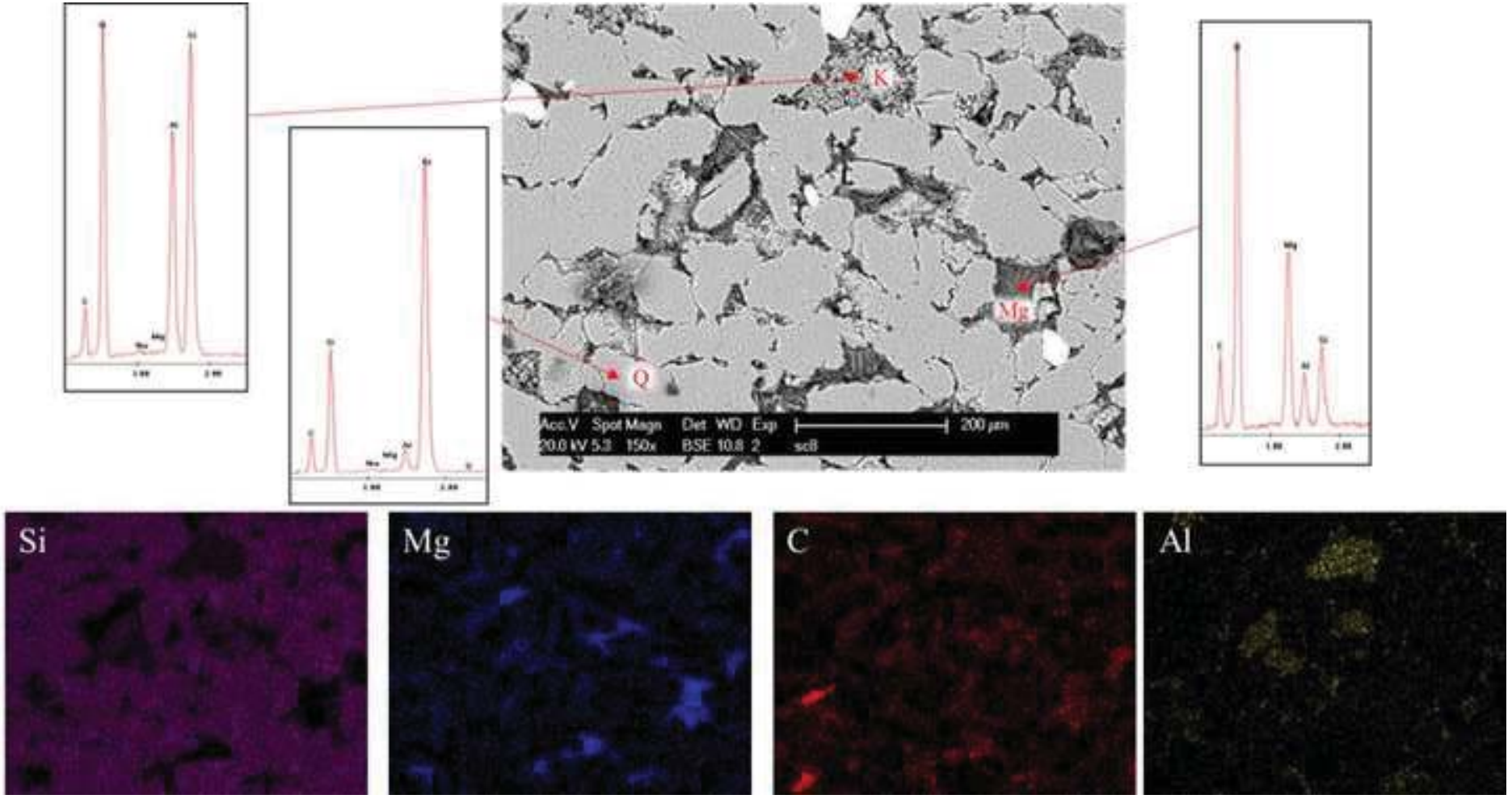

Table 1. Physic properties of sandstone which were determine following the European standards stated in the table and the methodology proposed in different studies.

Water accessible porosity [% v/v]	13.24 ± 0.31	RILEM 1980 [43]
Mercury accessible porosity [% v/v]	17.38 ± 0.25	
Capillary porosity [% v/v]	11.47 ± 0.25	
Capillarity coefficient C ($kg/m^2s^{0.5}$)	0.046 ± 0.001	ICR-CNR 1985 [44]
Saturation degree (by immersion) [%]	99.31 ± 2.17	ICR-CNR 1981 [45]
Saturation degree (by capillarity) [%]	87.58 ± 0.33	ICR-CNR 1985 [44]
Tortuosity	8.02 ± 0.25	[39]
DDE	3.69 ± 0.18	[40]
Zeta potential [mV]	-24 ± 9.61	

Table 2. Hg accessible porosity, tortuosity and DDE index of the untreated sandstone, of the sandstone subjected to steps 1 and 2 and of the treated samples subjected to the lixiviation test. Data obtained from samples taken near the cathode and near the anode are shown.

Code of Samples	Electrode	Accessible porosity to Hg (%)	Tortuosity	DDE
Reference	**Sandstone**	17.4	8.0	3.7
CT1	**Cathode**	16.0	6.1	2.1
	Anode	16.2	5.1	3.7
	Cathode Lixiviate	17.1	9.3	3.4
	Anode Lixiviate	17.4	11.4	3.7
CT2	**Cathode**	13.9	4.3	1.9
	Anode	16.2	4.3	3.5
	Cathode Lixiviate	15.0	5.6	3.3
	Anode Lixiviate	16.9	8.4	3.6

Springer

Disclosure of potential conflicts of interest

Authors must disclose all relationships or interests that could have direct or potential influence or impart bias on the work. Although an author may not feel there is any conflict, disclosure of all relationships and interests provides a more complete and transparent process, leading to an accurate and objective assessment of the work. Awareness of a real or perceived conflicts of interest is a perspective to which the readers are entitled. This is not meant to imply that a financial relationship with an organization that sponsored the research or compensation received for consultancy work is inappropriate. For examples of potential conflicts of interests *that are directly or indirectly related to the research* please visit:
springer.com/gp/authors-editors/journal-author/journal-author-helpdesk/before-you-start

Corresponding authors of papers submitted to Materials and Structures (name of journal) must complete this form and disclose any real or perceived conflict of interest. The corresponding author signs on behalf of all authors.

The corresponding author will include a statement in the text of the manuscript in a separate section before the reference list, that reflects what is recorded in the potential conflict of interest disclosure form. Please note that you cannot save the form once completed. Kindly print upon completion, sign, and scan to keep a copy for your files.

The corresponding author should be prepared to send the potential conflict of interest disclosure form if requested during peer review or after publication on behalf of all authors (if applicable).

☑ We have no potential conflict of interest.

Category of disclosure	Description of Interest/Arrangement
JORGE FEIJOO	FPU grant

Article title AN IMPROVED ELECTROKINETIC METHOD TO CONSOLIDATE POROUS MATERIALS

Manuscript No. (if you know it) MAAS-D-17-00269

Corresponding author name Jorge Feijoo

Herewith I confirm, on behalf of all authors, that the information provided is accurate.

Author signature [signature] Date 07/03/2017